A magnetotelluric model of the Mana Pools basin, northern Zimbabwe

JOURNAL OF GEOPHYSICAL RESEARCH, VOL. 105, NO. B5, PAGES 11,185–11,202, MAY 10, 2000

A magnetotelluric model of the Mana Pools basin, northern Zimbabwe

D. Bailey,[1] K. A. Whaler,[1] T. Zengeni,[2] P. C. Jones,[3] and O. Gwavava[2]

Abstract. The Mana Pools sedimentary basin lies within the Zambezi mobile belt in northern Zimbabwe. New and preexisting magnetotelluric data and the available seismic reflection data are used to constrain the basin structure and the depth to the electrical basement. Long-period magnetotelluric (LMT) data were collected at five stations along a 60 km north-south profile across the Mana Pools basin and onto the southern escarpment. These data augment an existing audiofrequency (AMT) data set from 11 sites in the same area. The subsurface apparent resistivities measured at periods sampling the basin are very low (a few Ωm). After processing both data sets, the estimated impedance tensor is decomposed, showing that the resistivity structure of the Mana Pools basin can be modeled two dimensionally. The ρ^+ algorithm is used to show that there is no systematic offset in magnitude between the AMT and LMT data sets before they are combined. Minimum structure resistivity models of the Mana Pools basin compare well with the information from reflection seismic data and support its previous description as a half graben basin of ~7 km depth. The excellent conductor in the Mana Pools basin is quite different to those seen elsewhere in the orogenic belt in that it is a feature of the sedimentary fill rather than the basement. The resistivity of the basement is low but no localized good conductor is observed; these low resistivities may result from a high degree of either chemical or tectonic alteration to the underlying rocks due to metamorphic processes and tectonic disruption during rift formation.

1. Introduction

The African continent has been largely divided into stable cratonic blocks and mobile belts during its tectonic history. This differentiation dates back to the end of the Archean period, but the mobile belts have a long and complex history of movement stretching to the end of the Pan-African orogeny, ~600 Ma. Subsequent rifting of the African continent between the late Permian and the early Tertiary led to the formation of a number of Karoo basins within the mobile belt terranes. DC resistivity soundings [e.g. *van Zijl*, 1977] taken in a variety of different tectonic settings indicate that there are a number of distinct resistivity layers which are continuous across large parts of the southern African continent. One of these layers is very conductive and occurs as a thin region at depths of ~40 km in cratonic blocks. It is also observed to be developed more strongly in mobile belt regions, where its upper surface is detected at shallower depths. Geomagnetic depth sounding (GDS) surveys [*de Beer et al.*, 1976, 1982] have detected this conductor as a continuous feature running from the Atlantic coast in Namibia and exploiting the Damara mobile belt to run across Botswana and connect with the Zambezi belt in the east (see Figure 1). Studies of this feature have concentrated mainly on the Damara belt, where the conductor's position has been mapped in more detail. Resistivity soundings [e.g. *de Beer et al.*, 1982] tend to favor an association between the conductor and the basement, although the conductor has been detected at only 3 km depth within the mobile belt [*van Zijl and de Beer*, 1983; *de Beer et al.*, 1982]. While the position of the conductor has been mapped in some detail, its origin remains a mystery.

More recently, both the Lower Zambezi and Mana Pools Karoo sedimentary basins (Figure 2) lying within the Zambezi valley mobile belt have been investigated. *Losecke et al.* [1988] detected an extremely good conductor at depth beneath the Lower Zambezi basin during a magnetotelluric (MT) survey carried out there. This may be linked to the feature seen by *de Beer et al.* [1975, 1976, 1982] and *van Zijl and de Beer* [1983] extending between the mid-Zambezi basin of the Zambezi mobile belt and the Damara orogenic belt to the west. The Mana Pools basin was investigated using audio-

[1]Grant Institute, University of Edinburgh, Scotland.
[2]Department of Physics, University of Zimbabwe, Harare, Zimbabwe.
[3]British Antarctic Survey, Cambridge, England.

Paper number 1999JB900434.
0148-0227/00/1999JB900434$09.00

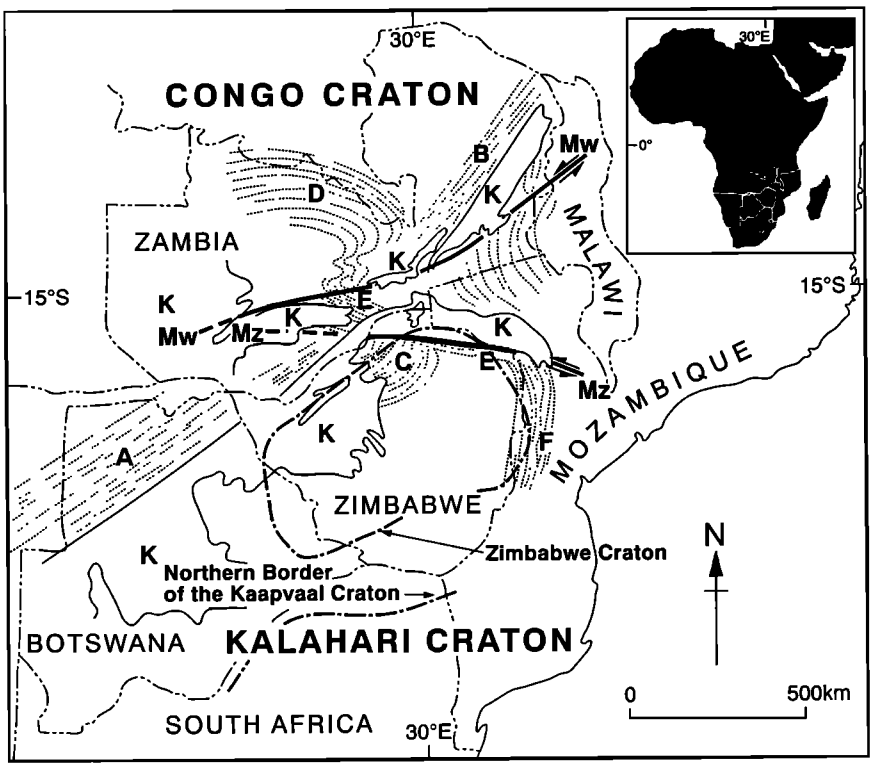

Figure 1. The mobile belts of central Africa, after *Orpen et al.* [1989]. The Karoo basins are marked with a K and the mobile belts are identified as A, Damaran; B, Irumide; C, Magondi; D, Lufilian Arc; E, Zambezi; and F, Mozambique. The Mwembeshi shear zone (Mw) and Mzarabani fault (Mz) are also labeled. The boundaries of the Zimbabwe and Kaapvaal cratons are marked with dot-dashed lines; that of the former is reproduced from *Ranganai* [1995].

frequency MT methods by *Whaler and Zengeni* [1993], who produced a preliminary resistivity model for the basin, but depth resolution was limited; however, they did establish that there is a good subsurface conductor. In this paper, the results of a follow-up survey in 1995 where longer period MT data were collected are included. The data from both surveys are robustly processed, the dimensionality of the structure they contain is examined, and a new two-dimensional resistivity model of the Mana Pools basin is presented. The results are compared with other geological and geophysical information, especially a reflection seismic survey [*Hiller and Buttkus*, 1996].

2. Geological and Geophysical Studies in the Zambezi Valley

The Pan-African orogeny occurred between 1100 and 600 Ma and was the last major tectonic event of the Precambrian to affect central and southern Africa [*Barber*, 1994]. It created a large number of mobile belts in central Africa (Figure 1), whose margins, following the final phase of convergence, are commonly defined by ductile shear zones [*Barber*, 1994]. The early stages of the orogeny, from 1100 to 667 Ma, involved 285° orientated pull-apart forces and completed the structural differentiation of the continent into cratonic and mobile belt environments. This phase created the Pan-African intracratonic and proto-oceanic basins in south and west Africa.

The main features controlling tectonic processes within the Zambezi valley are shown in Figure 1. The Kalahari and Congo cratons separated dextrally during the Pan-African orogeny along the Mwembeshi shear zone which runs NE-SW across the region [*Daly*, 1986]. This shear zone bounds the Zambezi belt to the west, while to the east the belt continues until it merges with the north-south trending Mozambique belt. The second major control on tectonics in the Zambezi valley is the Mzarabani shear zone which trends east-west across the area. *Daly* [1986] and *Coward and Daly* [1984] proposed that the southern margin of the Zambezi belt is a major thrust zone, which either coincides with the Zambezi escarpment or lies to the north of it beneath the Karoo cover. The estimated sinistral displacement along the Mzarabani shear zone is 150 km [*Orpen et al.*, 1989, hereafter referred to as OSNZ].

The Lower Zambezi, Mana Pools, and Mid-Zambezi basins lie within the Zambezi valley (Figure 2); their tectonic and structural development is described by OSNZ. The western boundary of the Lower Zambezi and eastern boundary of the Mana Pools basins are

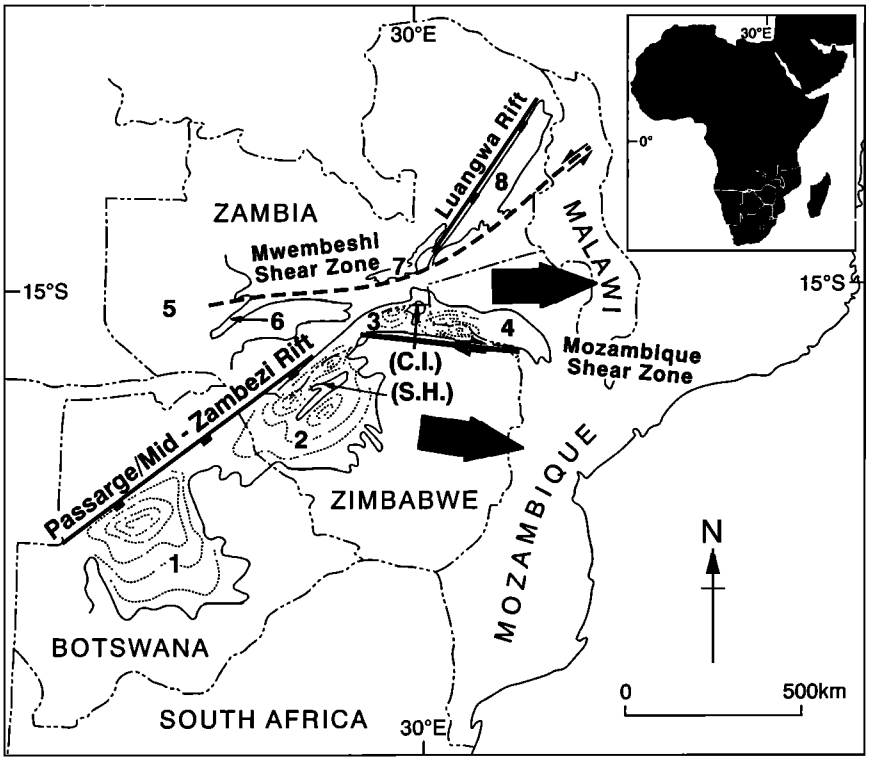

Figure 2. The central African Karoo sedimentary basins, after *Orpen et al.* [1989]. Approximate basement contours derived from potential field methods are shown and the basins are numbered: 1, Passarge; 2, Mid-Zambezi; 3, Mana Pools; 4, Lower Zambezi; 5, Western Zambian; 6, Kafue; 7, Luano; and 8, Luangwa. The Sijarira horst (S.H.) separates subbasins within the Mid-Zambezi basin, and the Mana Pools and Lower Zambezi basins are separated by the Chewore inliers (C.I.). Basins 3 and 4 are of interest here.

marked by the Chewore inliers (Figure 2). These form a horst of Precambrian rocks extending south from Zambia into the Karoo sediments of northern Zimbabwe. The Mana Pools basin has an estimated depocenter of 5 km from gravity and magnetic methods. The Lower Zambezi basin is bounded to the south by the Mzarabani fault. The major synsedimentary faults strike obliquely to it and downstep toward an ~10 km depocenter close to the southern margin. The northern margin of the basin is more complex. Satellite imagery reveals several northwest striking faults which splay off a main east-west escarpment fault. The Lower Zambezi basin therefore has an asymmetric profile with the basement sloping down to the south.

The evolution of the Mana Pools basin, at the intersection of the Lower Zambezi and Mid-Zambezi rift systems, is not understood; satellite imagery shows that the Mzarabani Fault continues westward from the Lower Zambezi basin to bound the southern margin of the Mana Pools basin. The NNW margin of the Mana Pools basin is also fault bounded; satellite data show that the marginal fault splays off the Luangwa trough system west of the Chewore inliers and runs along the margin of the basin. The tectonic controls on the Mana Pools basin remain unknown, although the geometry of the basin suggests that it is a half graben.

Some of the ambiguities in the interpretation of the basin structure were resolved following a reflection seismic survey by Mobil Exploration Zimbabwe Incorporated [*Hiller and Buttkus*, 1996]. The Mana Pools basin seismic data were collected in two profiles across its western portion, since much of the center of the basin lies within a World Heritage Site, but their interpretation is thought to be representative. The simplified geological structures of the Lower Zambezi and Mana Pools basins are shown in Figure 3, based on the seismic interpretation of the profiles shown on Figure 4(a). The depth to the seismic basement is well constrained by the data, which suggest, for the Mana Pools basin, a graben-like structure though slightly deformed and displaying a warped basement. The warping of the basement seems to have deepened the basin adjacent to the southern escarpment creating a second shallower depocenter. The northern depocenter is 7 km deep which is in reasonable agreement with OSNZ's value of 5 km. The depth to basement in the Lower Zambezi basin, ~12 km, is also in good agreement with the estimate of OSNZ.

Prior to acquisition of the seismic data, the discovery of a zone of high electrical conductivity [*de Beer et al.*, 1976, 1982] which, it has been suggested, links the Damara belt with the Zambezi belt to the east, was

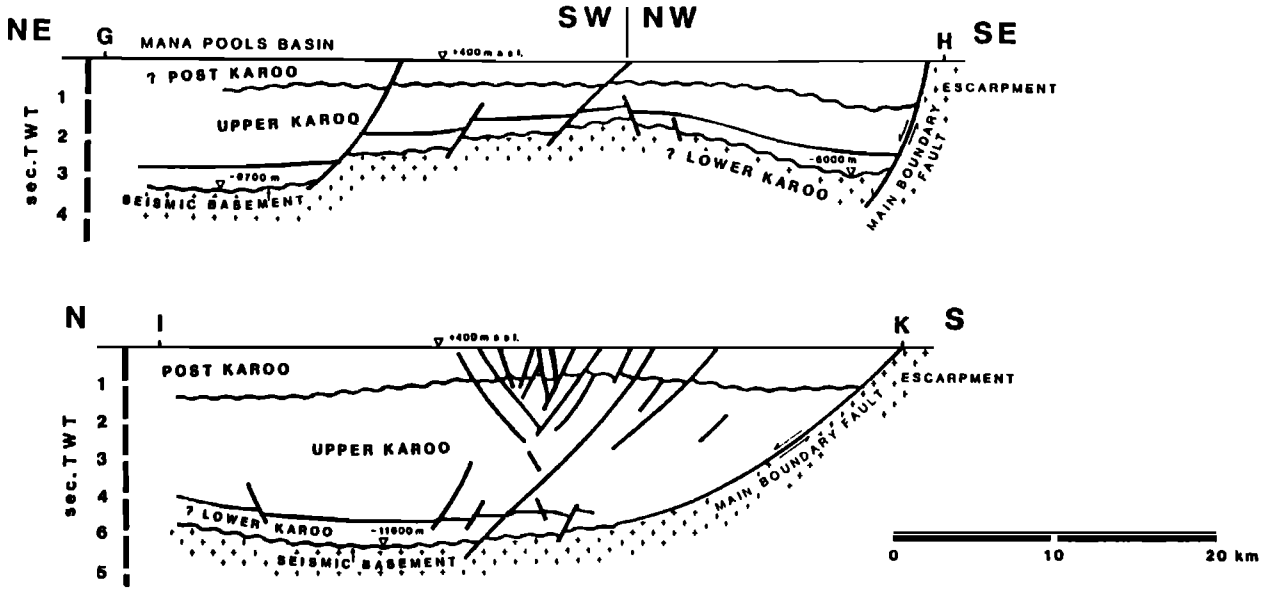

Figure 3. The structure of the Zambezi valley basins, interpreted from reflection seismic data, after *Hiller and Buttkus* [1996]. Top, Mana Pools; bottom, Lower Zambezi.

followed by a number of electrical and electromagnetic studies in the Zambezi valley. Many of these studies are discussed by *Haak and Hutton* [1986]. In 1988 a MT survey of the Lower Zambezi basin was undertaken by *Losecke et al.* [1988] (hereafter referred to as LKM) along north-south profiles at periods between 0.2 and 2000 s, extending to 10,000 s at some sites. A two-dimensional model along the profile of the Lower Zambezi basin of Figure 4 proposed from forward modeling studies by LKM is shown in Figure 5. There are three zones to the model; zone 1 is a good conductor of resistivity 2 to 10 Ωm extending to between 1 and 4 km deep and thinning southward toward the Zambezi escarpment. Zone 2 is much more resistive, typically 1000 Ωm and between 2 and 12 km thick; its maximum thickness is adjacent to the southern escarpment, and it tapers severely to the north. Zone 3 is an extremely good conductor of resistivities to below 0.5 Ωm. LKM claim that zone 3 continues to a depth of 30 km and that its base is not resolved. The depth and resistivity of zone 3 increase to the south and the west as the escarpment and Chewore complex, respectively, are approached; this may indicate a change in the conductor's nature (LKM). The contrast between the electrical structure on the Zimbabwe craton and that in the mobile belt is evident in Figure 5. The cratonic rocks are much more resistive; the model has values of 8000 Ωm to a depth of at least 20 km.

LKM, with the help of existing potential field data, interpreted zone 1 as consisting of nonmetamorphic sediments of post-Karoo and Karoo age. Zone 2 was thought to be either the upper part of the crystalline basement or a layer of consolidated sediments containing intercalated basalt sills. The resistivity and density of these two rock types overlap considerably making them indistinguishable by these methods (LKM). The latter explanation is preferred in light of the seismic results. It is difficult to hypothesise a cause of the extremely low resistivities of zone 3 and similar conductive zones elsewhere in the Damara orogenic and Zambezi mobile belts. The seismic data indicate that the Lower Zambezi conductor lies at basement depths which makes its low resistivity remarkable. This could be explained if the basement resistivity has been reduced by deformation or is of a different material to that comprising the craton (LKM).

Following the MT survey of the Lower Zambezi basin, the Mana Pools basin was also surveyed using MT methods [*Whaler and Zengeni*, 1993, hereafter referred to as WZ]. Audiofrequency magnetotelluric (AMT) data (frequencies 0.016 to 128 Hz) were collected at 11 sites along a north-south profile extending 40 km from the Zambezi River in the north to the Zambezi escarpment in the south (Figure 4). Again, a large contrast was observed between the resistivity of the southern craton and that within the basin. The craton was modeled with values of 2000 to 3000 Ωm, while the basin consists of a variable thickness low-resistivity (a few Ωm) layer up to 10 km thick, over a 10 Ωm layer possibly representing the geological basement (WZ). If the identification of the geological basement is correct, which the seismic data subsequently obtained suggest it is, then its resistivity is low even for a mobile belt with such a long history of movement. WZ tentatively interpreted the overlying layer as a sedimentary succession with variations in resistivity being identified with different stratigraphic units. Using the D^+ algorithm [*Parker*, 1982], they showed that within the basin the

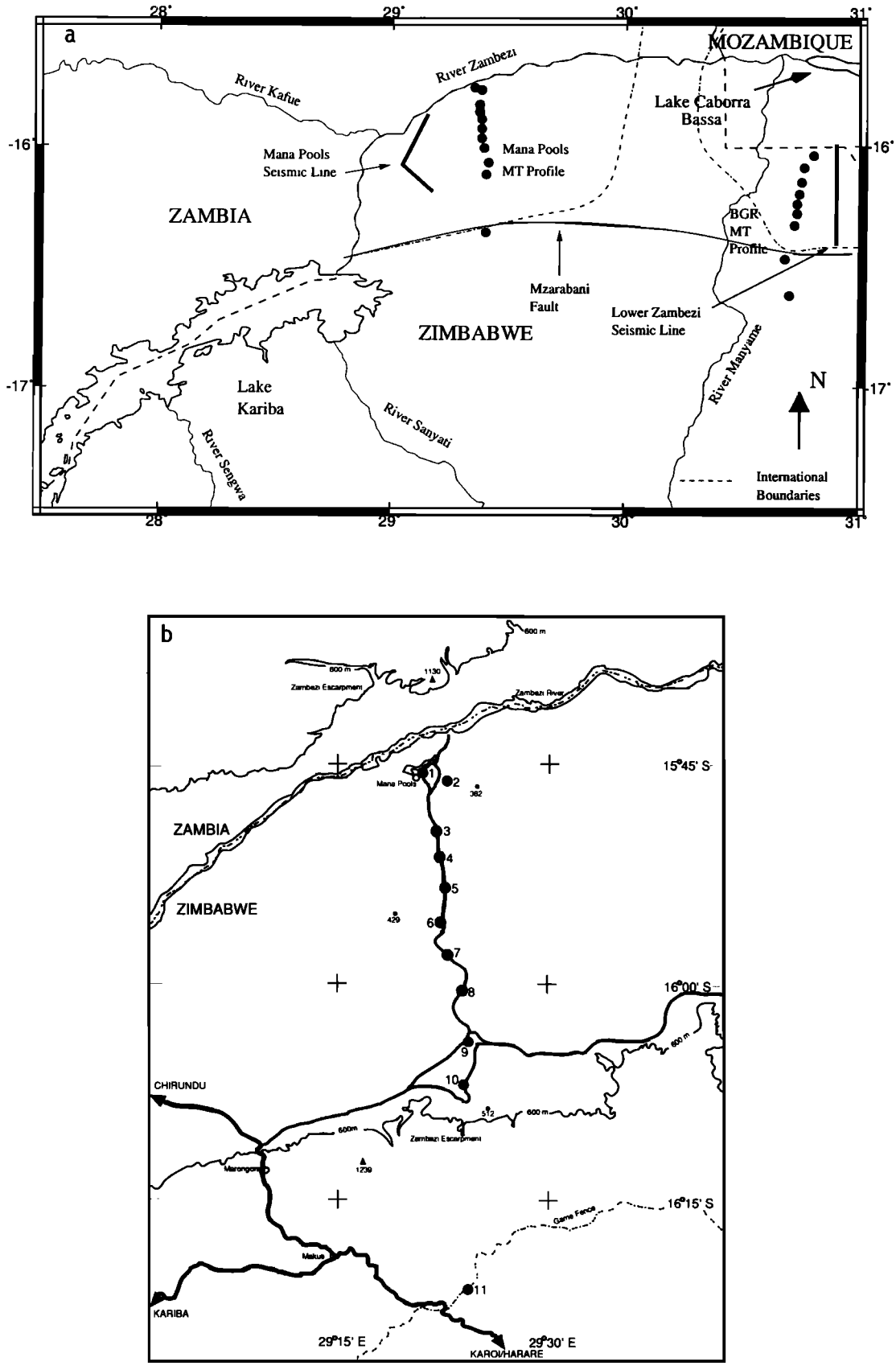

Figure 4. (a) The Mana Pools and Lower Zambezi areas, showing the MT sites (dots) and seismic profiles (thick lines). Dot-dashed lines mark the extent of the basins; dashed lines show the international borders. (b) Details of the Mana Pools MT survey. Numbers indicate sounding sites. LMT data were collected at sites 1, 6, 8, 10, and 11. After *Whaler and Zengeni* [1993].

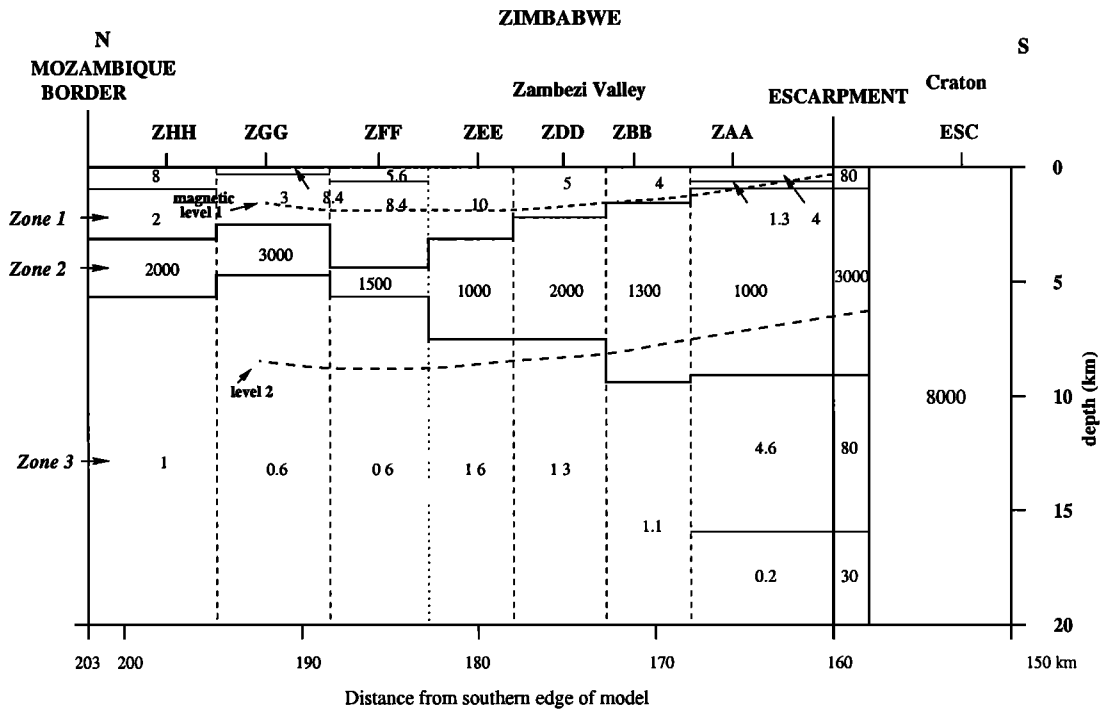

Figure 5. Two-dimensional resistivity model of the Lower Zambezi basin; figures indicate resistivity in Ωm, after *Losecke et al.* [1988]. The magnetic levels represent the two magnetic horizons observed in the aeromagnetic survey [*Bosum and Geipel*, 1988].

sediment-basement interface is just at the resolution depth of the data and therefore may not be properly determined. For this reason, long-period magnetotelluric (LMT) data were also collected in 1995 at sites 1, 6, 8, 10, and 11 (Figure 4(b)). We used EDA fluxgate magnetometers and silver-silver chloride electrodes separated by 100 m, collecting data for up to 5 weeks at a sampling rate of 20 s, with a band pass of between 40 and 3000 s. The data collected in both field campaigns were processed, and impedance tensors relating the measured electric and magnetic fields as a function of frequency were determined using the *Egbert and Booker* [1986] robust time series processing algorithm and a single-site approach. These impedance tensors depend on the resistivity distribution of the subsurface and are used to determine the electrical structure at depth.

3. Distortion of the Impedance Tensor

The structure of the impedance tensor is characteristic of the dimension of subsurface structure it describes. For a one-dimensional Earth the impedance tensor has elements $Z_{xx} = Z_{yy} = 0$ and $Z_{xy} = -Z_{yx}$. The former condition also holds for a two-dimensional Earth providing that the electric and magnetic field measurements are made perpendicular and parallel to electrical strike. This condition can be satisfied during processing by simply rotating the tensor into the required coordinate system [e.g., *Swift*, 1967]. For a three-dimensional tensor all elements are nonzero. Note these conditions are all necessary but not sufficient: A tensor obtained over a three-dimensional structure can have small diagonal elements, for instance. The situation is complicated by small near-surface conductivity anomalies with a galvanic but no inductive response: these bodies can distort the structure of the measured impedance tenor [e.g., *Jones*, 1983], and their effect must be removed.

An indication of the dimensionality of the impedance tensors prior to modeling is given in Figure 6 which shows the results of a Bahr classification [*Bahr*, 1991] of the Mana Pools data set; the numbers plotted are the Bahr class to which each impedance tensor at each frequency belongs. The majority of the data fit a two-dimensional model distorted by small heterogeneities with only a galvanic response (classes 3 to 5) [*Bahr*, 1991], the class value reflecting the degree of distortion. The data at periods expected to be sampling the sedimentary basin are generally only weakly distorted, while those to the south and at longer periods show stronger galvanic distortion. There are very few significant periods of class 7 data, which indicate three-dimensional structure. They are in regions where the signal-to-noise ratio is low and the data are believed to be of poor quality, so the high class number may be reflecting this rather than genuinely three-dimensional structure. With data from a single profile we are unable to investigate the extent to which the structure is three-dimensional.

A standard approach outlined by *Bailey* [1998] was used in the analysis of all the impedance tensors in

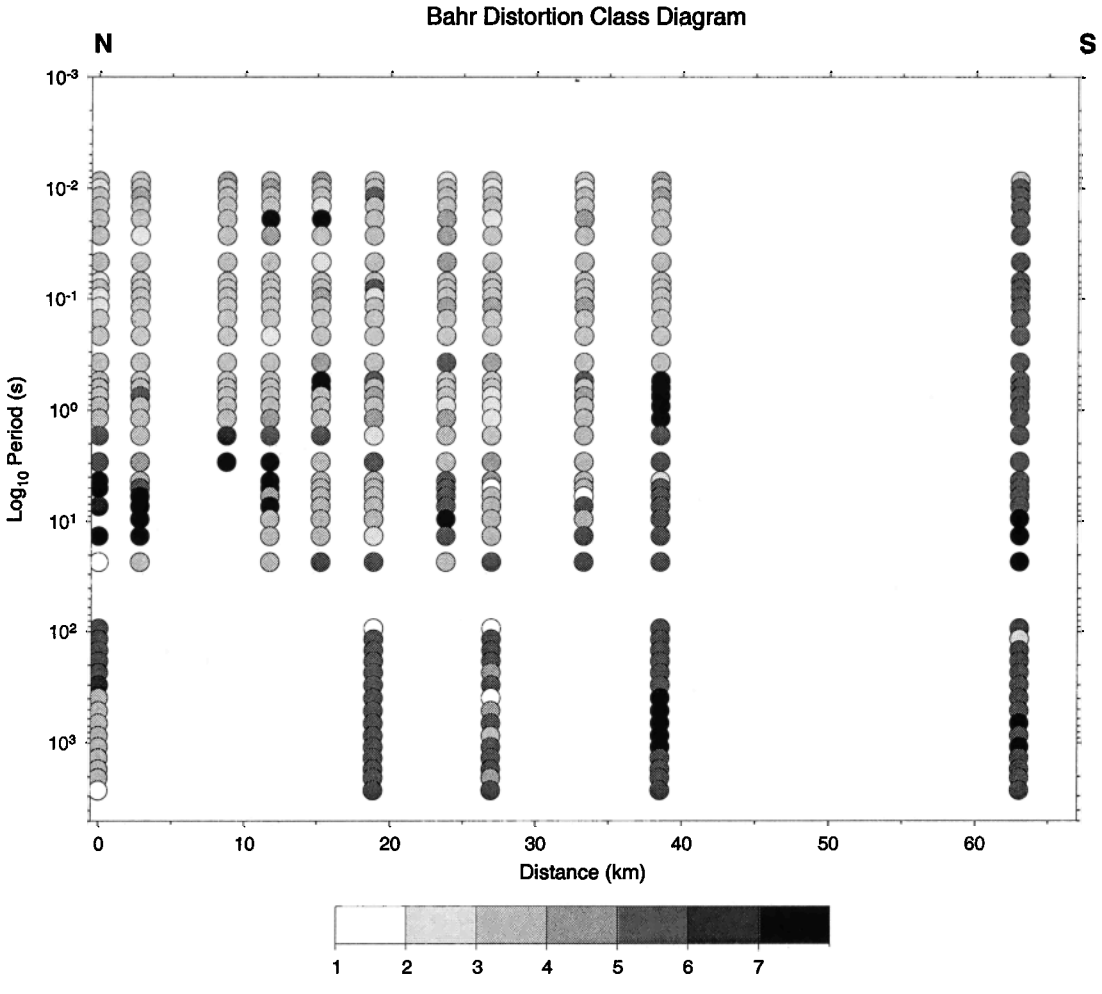

Figure 6. The *Bahr* [1991] distortion class results.

the Mana Pools data set. The appropriateness of the *Groom and Bailey* [1989] decomposition was assessed by comparing its error of fit with that of the simpler two-dimensional decomposition of *Swift* [1967] and by assessing the frequency independence of the distortion parameters. A significant reduction in misfit was required for the Groom and Bailey (hereafter referred to as GB) decomposition to justify the extra parameters it contains. If this was the case, the decomposition's validity was checked by attempting to constrain the distortion parameters over a certain frequency range; this should result in no significant increase in the error of fit to the data. The constrained distortion model was considered to be valid provided the following criteria were satisfied: (1) It had a misfit lower than a model requiring fewer parameters (i.e., the Swift decomposition) and not significantly greater than that for the unconstrained distortion model, (2) the distortion parameters were frequency-independent over a frequency range of at least one decade, and (3) the apparent resistivity and phase curves were smoothly varying and consistent with those at neighbouring sites [*Groom and Bailey*, 1989].

The results of the constrained GB decomposition for site 6 are shown in Figure 7 as an example. Error bars are one standard deviation, calculated by Monte Carlo simulation during decomposition. For all sites the relative error of fit between the data and the model impedance estimates was smaller for the constrained GB distortion model than for the Swift model, typically by an order of magnitude. This was true throughout the entire period range except at periods between 1 and 400 s where the impedance estimates were so poorly constrained that they could be fit within their uncertainties at any regional azimuth. The GB decomposition gives a good fit to each element of the measured impedance tensor at all sites, the only exception being the AMT frequency range at site 11 (Figure 8), where twist and shear are large, around -15° and 30°, respectively, and Figure 6 shows that the tensors at this site are strongly distorted. The apparent resistivity curves appear to be static shifted in the AMT period range, and there is also an offset in the LMT apparent resistivity at ~400 s. This period marks the transition from noisy data to better constrained data, and clearly, the

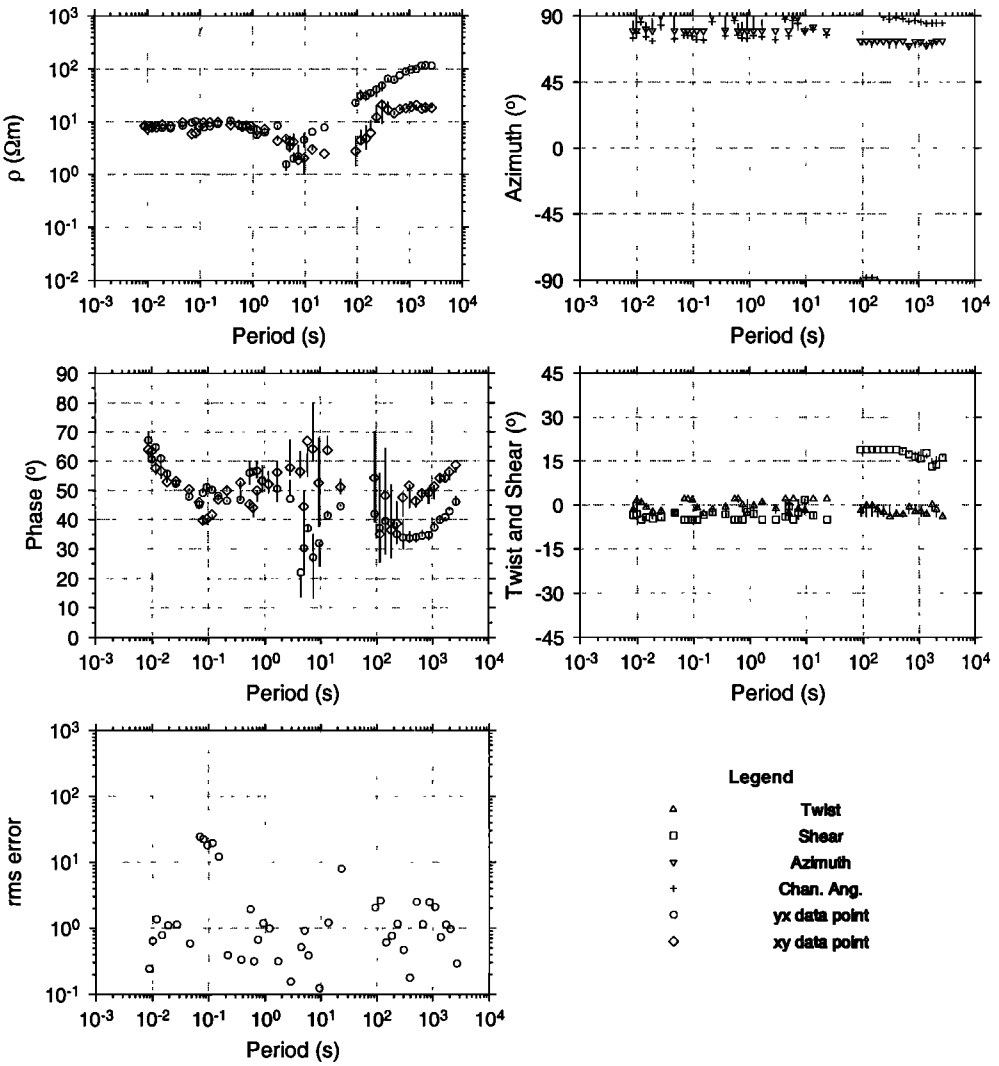

Figure 7. The results of the constrained *Groom and Bailey* [1989] decomposition for site 6. Error bars here and in subsequent plots are one standard deviation. The regional azimuth has been set to 80°.

impedances at this site between 100 and 400 s are not sufficiently constrained to be meaningful.

Frequency independence of the distortion parameters is achieved very satisfactorily for the LMT data at all sites barring site 8, where the data are too poor to justify the application of constraints. The regional azimuth is seen to vary from approximately east-west to north of east as the sites are traversed from north to south and has been set to 80° at all sites for subsequent inversion. Twist and shear are relatively consistent in the LMT period range between sites within the valley; no significant change occurs until site 11, but the distortion parameters are significantly different between the AMT and LMT data sets. The local strike direction is extremely consistent for the LMT data within the valley, lying approximately east-west. The misfit of the LMT data increases from north to south, indicating greater three-dimensional induction. This may be due to the increasing proximity of the escarpment and a shallowing of the basin to the south. The conductive sediments in the valley will act to channel the current, and therefore, at longer periods, where the valley is no longer long or straight enough to be approximated two-dimensionally, strong three-dimensional current channeling effects can be encountered [*Groom and Bahr*, 1992]. The northward rotation of the local strike seen at the most southerly site within the basin is indicative of current channelling into the valley. Site 11 is on the resistive side of the Zambezi escarpment, and the electric field is distorted by currents deviating northward to flow into the more conductive basin, altering the local strike and increasing the magnitude of the distortion parameters.

Before modeling, the AMT and LMT data sets have to be amalgamated. This is problematic owing to a gap of just over a decade between the periods of the data from the two surveys. It is therefore difficult to assess whether there is a systematic mismatch in the appar-

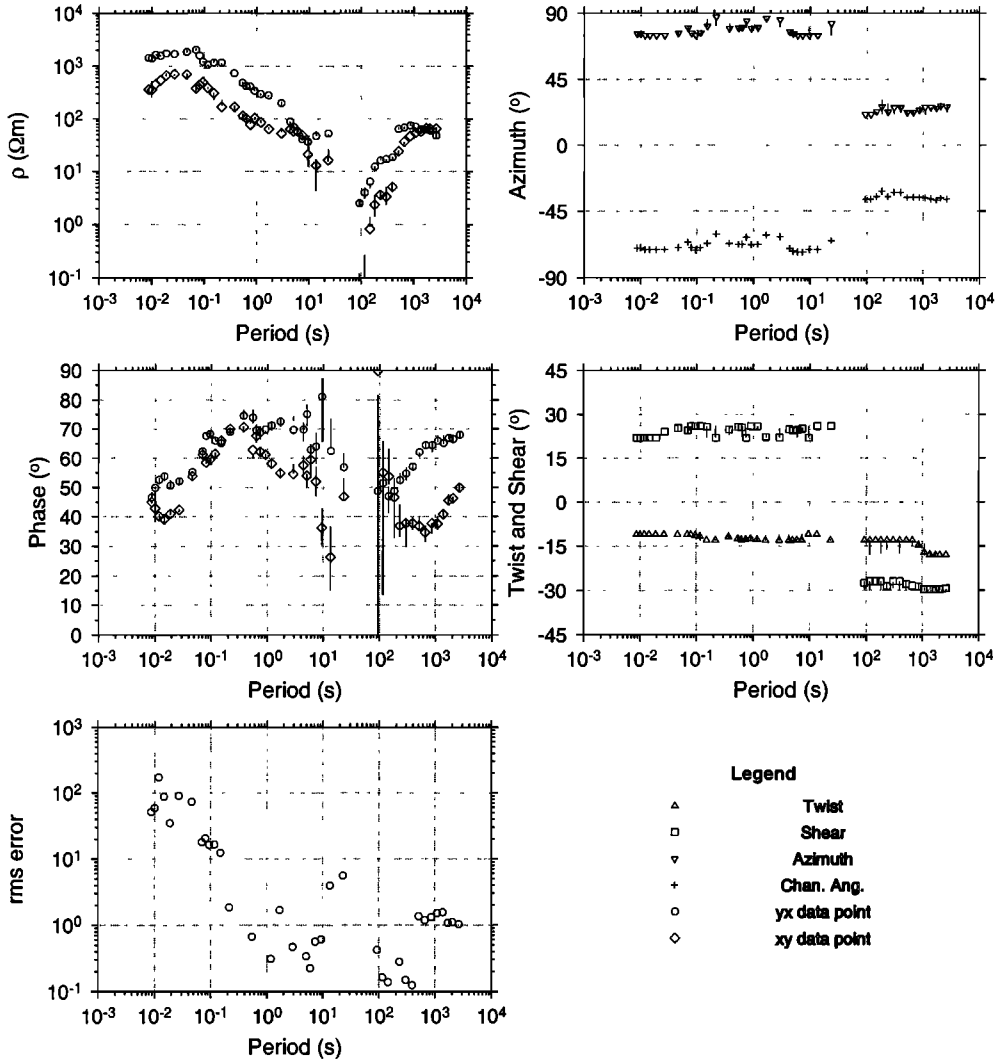

Figure 8. The results of the constrained *Groom and Bailey* [1989] decomposition for site 11.

ent resistivity magnitude between the data from the two period ranges. To overcome this problem, the ρ^+ code [*Parker and Booker*, 1996] is used as described by *Bailey* [1998] to check the consistency between the AMT and LMT data. The ρ^+ algorithm finds the best fitting one-dimensional resistivity model to a collection of MT apparent resistivity and phase data. *Parker and Booker* [1996] have used the work of *Weidelt and Kaikkonen* [1994] to apply this technique further to the H polarization data from a two-dimensional structure. Here we make the assumption of two-dimensionality based on the results of the *Bahr* [1991] class analysis and assess the consistency of our H polarization (in which the magnetic field is orientated parallel to strike) combined data set using the ρ^+ technique. The best fitting ρ^+ model was obtained, and the maximum permissible variation of each apparent resistivity and phase datum from its predicted value was calculated subject to the condition that the misfit of the resulting model to the data set was not increased by more than two standard deviations. For all sites except 11 a good fit to the H polarization data with no systematic offset between the AMT and LMT data was achieved by simply rejecting points of low coherency between ~1 and 400 s, the longest periods in the AMT data and the shortest periods in the LMT data. It was observed that all the rejected points have downward biased apparent resistivity values compared to those predicted. We concluded that there is little or no mismatch between the two data sets and that they can be combined without adjustment. The exception is site 11, where no ρ^+ model provides an acceptable fit to the data, the apparent resistivity curves at this site indicating the presence of a static shift which is addressed in section 4.

4. Two-Dimensional Modeling

Rapid relaxation inversion (RRI) [*Smith and Booker*, 1991] is used to model two-dimensionally the GB decomposed data. This minimizes a combination of the

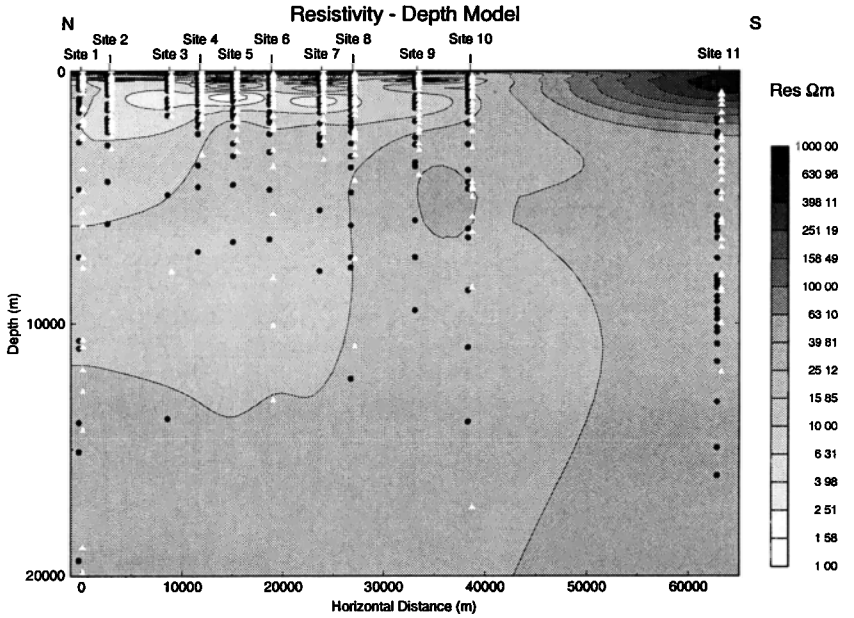

Figure 9. The resistivity structure of the Mana Pools basin derived from H and E polarization data. Triangles and circles represent H and E polarization data points plotted at one skin depth respectively.

fit to the data and a measure of lateral and vertical smoothness of the model. The model is parameterized on a grid conforming to the guidelines given by *Booker* [1997] with a total depth and width of ~600 and 300 km respectively, consisting of 71 nodes vertically and 93 laterally. Prior to inversion, the E and H polarization data are weighted by their associated one standard deviation errors so that undue weight is not given to poor data. The data are inverted as advocated by *Booker* [1997] using least squares iterations and subsequently applying Huber weights; redescending weights are then employed which downweight large outliers more severely. Finally, once the minimum (or a specified target) misfit is achieved, further iterations, as many as have previously been completed to reduce the misfit, are performed purely to smooth the solution.

A particular consideration in inverting this data set is the effect on the model of the difference in the period range at different sites, only five of which have LMT data, and of the differences in recording equipment used in the two surveys. One of the advantages of RRI is the ability to vary the χ^2 misfit goal between sites. The facility is used here to try to balance the inversion of sites with data for the entire frequency band and those with only AMT data. Each site is fit to the higher χ^2 misfit value achieved during separate inversions of the E and H polarization data. In this way, the fit to the two modes is even, and the model does not fit any site more tightly than is justified.

The data are inverted in a four-stage procedure similar to that laid out by *Livelybrooks et al.* [1993]; for details, see *Bailey* [1998]. Prior to inversion, extreme outliers are rejected, and data of low (< 80%) coherency are downweighted. This affects a large proportion of the data in the period range ~1 to 100 s, comprising the data in the MT dead band and at the long-period extremity of the AMT data, and also the first half decade of the LMT data which appear from the ρ^+ study to be downward biased. The resistivity structure obtained when both the E and H polarization modes were inverted simultaneously is shown in Figure 9; this has an rms misfit to the data of 1.71. The skin depth estimates plotted are calculated under the assumption of an overlying layer of homogeneous resistivity, equal to the apparent resistivity at that frequency. There are three main points to be noted from the model shown in Figure 9. First, there is a very conductive (resistivities as low as 2 Ωm) structure down to a depth of between 5 and 10 km, thinning and becoming less conductive to the south, which is in good agreement spatially with the position of the basin defined seismically [*Hiller and Buttkus*, 1996] and by gravity and magnetic data (OSNZ). Second, the surface layer at site 11, on the craton, is resistive to a maximum depth of 3 km. Third, beneath this, and below the basin in the valley, the basement has relatively uniform (between 20 and 30 Ωm) resistivity. This last observation is less certain than the previous two. There are reliable LMT data penetrating to below 25 km, but the depth range from ~8 to 20 km is beyond the penetration depth of most of the AMT data and is badly affected by low coherency at the LMT sites. Therefore the amount of data constraining the structure in this region is small, and the uniformity of resistivity may be solely a feature of the RRI smoothing process. This model can be compared with that of WZ, who stitching together one-dimensional models,

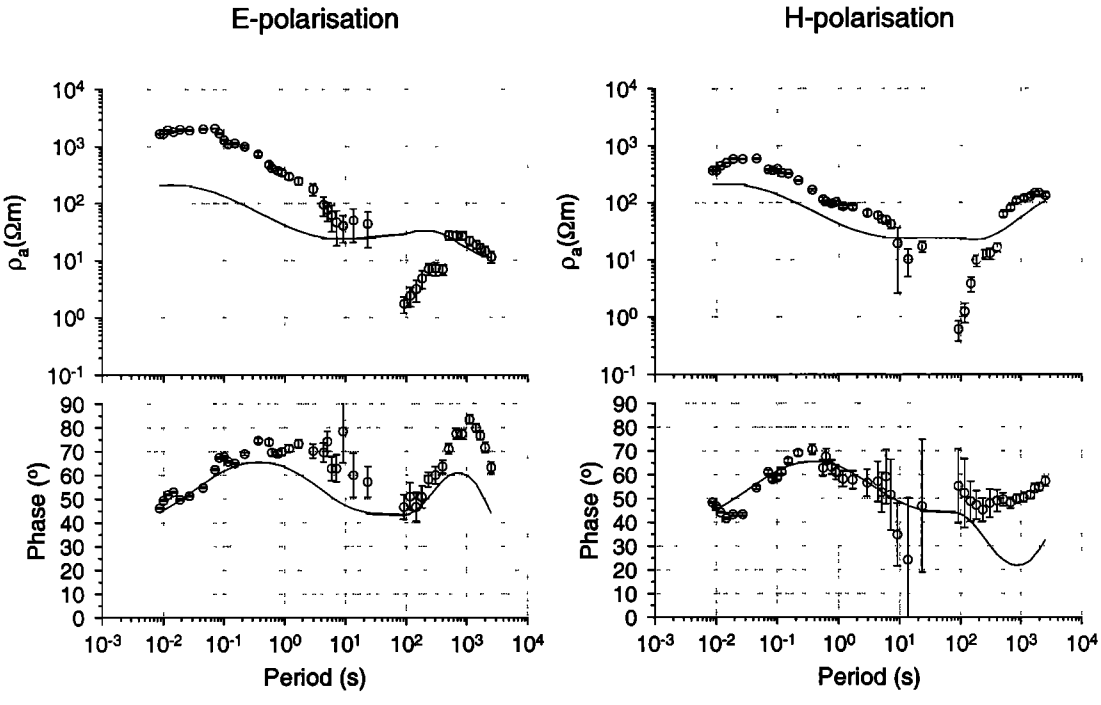

Figure 10. Fit to the data from site 11 when only phase data were included in the inversion. Circles represent data points decomposed at a strike angle of 80°, and the lines represent the response of the model.

produced a three-layer basin structure. Their resistivity section comprised a ~10 km section of variable resistivity overlying a conductive basement. This kind of layering is not seen in the model shown in Figure 9 and is therefore not required by the data. This is perhaps to be expected as there are significant deficiencies in the WZ model, as it was constructed from Berdichevsky average estimates of the impedance tensors calculated from nonrobustly processed data. There is reasonable agreement between the estimates of the depth to basement given by WZ and that shown by the model in Figure 9. However, WZ find a contrast between the resistivity beneath site 11 and that in the basin at all depths, which is not seen in Figure 9. While this may be due to a lack of depth penetration, particularly for the WZ model, it is also due to the contrast between stitched one-dimensional models and a two-dimensional minimum structure model and the effects of static shift at site 11. The model presented here is thought to be a more reliable representation of the resistivity structure.

Artificial jumps in the data can lead to artificial structure within the model. The decomposed data commonly show a drop in phase across the dead band (e.g., periods around 1 to 10 s in Figure 7); this ties in well at most sites with the observed drop in coherency. Beyond the dead band the phase is seen to climb again toward the end of the AMT period range. A similar pattern is also seen for the noisy shorter period portion of the LMT data at some sites. If these data were not downweighted, they would introduce a resistor and a deeper conductor in the model at a depth which corresponds approximately to the period gap between the two data sets. Deep conductive structures have been modeled or observed at basement depths in Pan-African mobile belts by other authors, for instance beneath the Lower Zambezi basin by LKM, also using MT data, and in a zone extending from the Damara orogenic belt in Namibia to the Zambezi mobile belt of Zimbabwe using DC resistivity and GDS array techniques by authors including *de Beer et al.* [1975, 1976, 1982] and *van Zijl and de Beer* [1983]. Such a deep conductive structure cannot be justified for the Mana Pools basin on the basis of our MT data since it relies on the inclusion in the inversion process of poor quality data. We cannot, however, rule it out.

The near-surface resistivity at site 11 is much higher than in any other part of the model and may be an artifact of static shift within the data. To assess this, an inversion was performed without the apparent resistivity data from site 11, which converged to an rms misfit of 1.58. This improvement in fit over the model of Figure 9 is due mainly to a reduced misfit at site 10, but the model also fits all of the LMT data better, although the misfit to the LMT apparent resistivity data is still significant. Structurally, the new model is similar to that of Figure 9. Figure 10 shows a plot of the apparent resistivity and phase data from site 11 with the predictions of this new model. The model fits the phase data well in terms of the shape of the two curves, and there is a reasonable fit to the phase magnitude for the

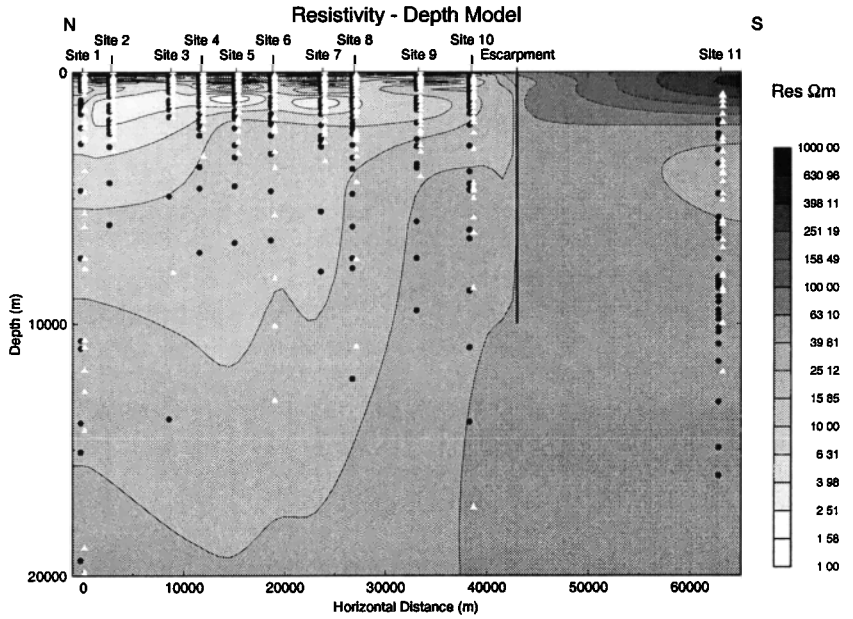

Figure 11. The resistivity structure of the Mana Pools basin derived with an escarpment fault extending to 10 km depth.

H polarization mode within the AMT frequency band. Neglecting the poor quality data, both LMT and AMT apparent resistivities are seen to be underestimated by the model. This underestimation is greater for the E polarization but is approximately frequency-independent for both polarizations. This strongly suggests an upward static shift on both polarizations which may be more severe for the E polarization. All further modeling is performed using only the phase data at site 11.

To test the consistency between the resistivity and seismic results and to see if the MT model can be modified to more closely match the seismic structure without compromising the misfit, more complex models were developed. A fault separating the sedimentary basin from the Zimbabwe craton to the south was included in the RRI inversion by allowing a resistivity discontinuity at the escarpment such that a jump across it does not cause any resulting penalty in the smoothness measure. The escarpment is between sites 10 and 11, and the seismic results of *Hiller and Buttkus* [1996] in Figure 3 show the fault reaches to a depth of at least 7 km with a steep dip to the north. It was implemented as

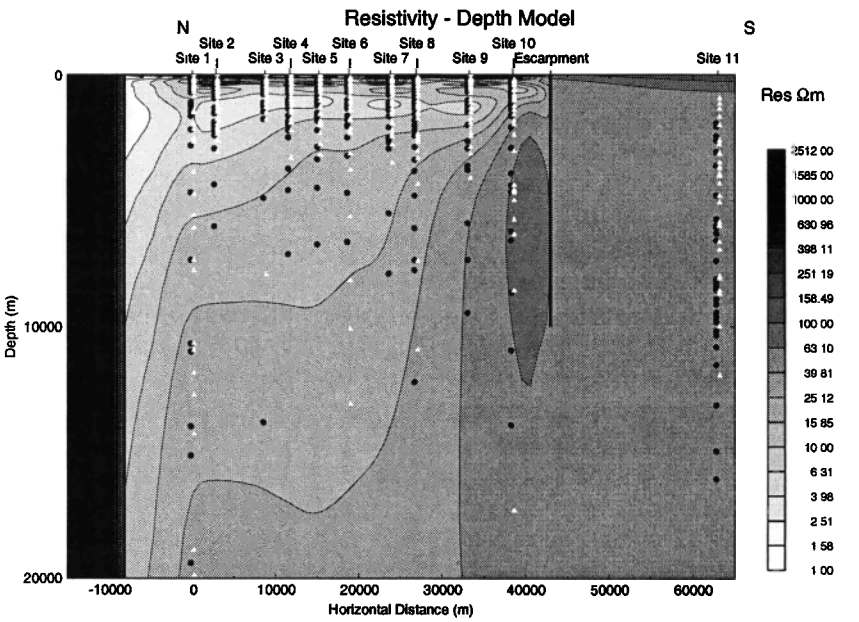

Figure 12. The resistivity structure of the Mana Pools basin derived with the addition of a second escarpment fault. The region plotted north of site 1 has been extended to show the position of the northern escarpment.

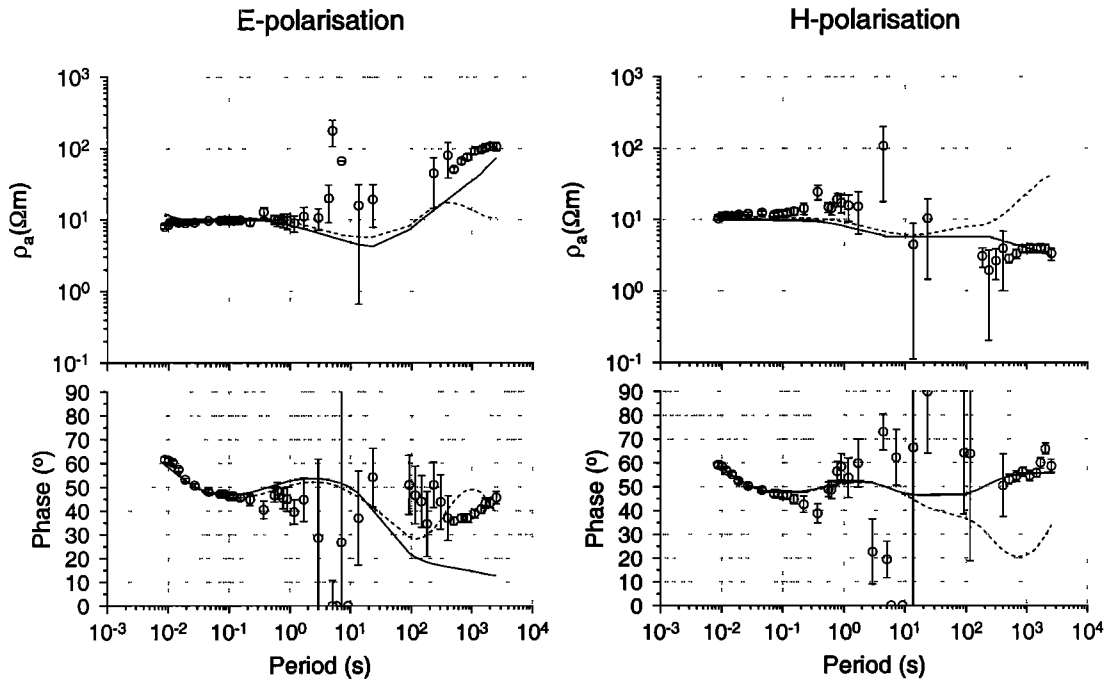

Figure 13. The fit of the models to the data from site 1. The solid line is the forward response of the model from Figure 12, and the dashed line is that of the model of Figure 11.

a 10 km vertical discontinuity, and Figure 11 shows the resistivity structure from the resulting inversion, which converged to an rms misfit of 1.39. This model still shows a systematic misfit to the LMT data at all the basin sites. The increasing separation between the E and H polarization LMT apparent resistivity data from south to north is similar to the behavior of the MT data of LKM for the Lower Zambezi basin as the proximity to the southern escarpment fault increases. It is this aspect of the behavior of the LMT data that the models are unable to replicate. There is a second escarpment in Zambia bounding the northern edge of the Mana Pools basin. It lies ~10 km to the north of site 1 and is a major structural feature, represented at the surface by a rapid increase in topography of over 600 m (Figure 4). This feature was introduced into the model as a vertical fault extending for the full depth of the model, separating the basin from a region with a resistivity of 2000 Ωm. This resistivity is of the same order of magnitude as that found for the craton south of the Lower Zambezi basin by LKM. The model obtained is plotted in Figure 12 and has an rms misfit of 1.26. The improvement in misfit may be a consequence of the addition of another break in the matrix representing the smoothness measure, but the fit to the data is better across the LMT period range than in previous models. Attempts were made to vary the depth at which the fault terminated, but these resulted in numerical instabilities, and the inversions were in all cases unsuccessful (see *Bailey* [1998] for further details). Figures 13 to 17 show the comparative fits to the data of the models shown in Figures 11 and 12, i.e., without and with a northern escarpment fault, respectively. It can be seen that for the sites overlying the basin and shown in Figures 13 to 15 the model in Figure 12 (solid) fits the data from both modes much better than that for the model in Figure 11 (dashed) with the exception of the E polarization phase data. The important observation is that while the exact magnitude of the apparent resistivity data is not matched, the fit to the shape and trend of the data is much better with the second escarpment fault added. Attempts were made to fit the data more accurately by varying the resistivity of the northern escarpment. As the resistivity was increased, the fit to the E polarization apparent resistivity data improved, but the fit to the phase data deteriorated and vice versa when the resistivity of the escarpment was decreased. An escarpment resistivity of 2000 Ωm offers a compromise in which both responses are fit to a reasonable degree [*Bailey*, 1998].

Figures 16 and 17 show the fit of the one and two escarpment models to the data from sites 10 and 11. Remembering that owing to static shift the apparent resistivity data from site 11 are not inverted, the pattern of the fit of the two models is similar to that in Figures 13 to 15 with both the E polarization phase and apparent resistivity data poorly predicted. The discrepancy between the models and the data at these two sites is also due to the difference between the 80° data decomposition angle and their preferred strike direction derived from the GB decomposition. It can be seen in Figure 17 that the frequency independence of

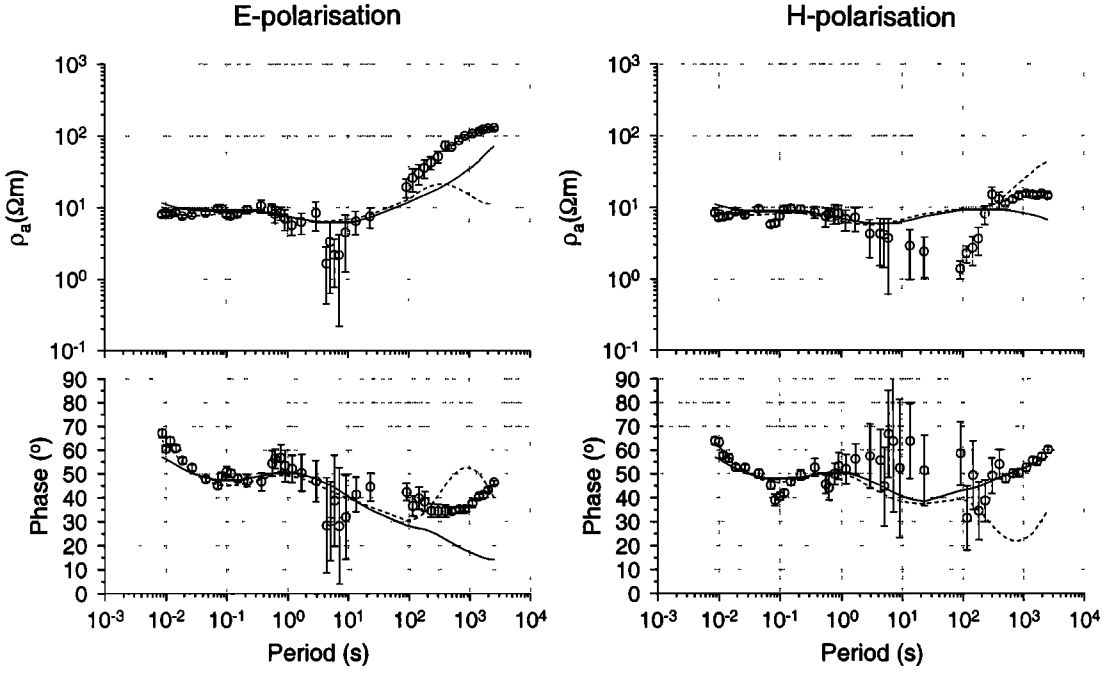

Figure 14. As for Figure 13, but for site 6.

the shift between the model apparent resistivity curve and the data for site 11 is lost for the model with two escarpments, and the fit to the phase data is particularly poor. This explains the difference in structure beneath site 11, the reduction in thickness and resistivity of the near surface layer, when the second escarpment is introduced. Also, a slightly more resistive feature appears beneath site 10 extending to the southern escarpment. Changes in structure elsewhere are considerably more subtle. Thus the most significant changes to the model when a second escarpment is added are beneath the two sites farthest from it. This reflects the strong nonlinearity of the MT inverse problem and the trade-off in contribution to the misfit from the various sites and the smoothness measure to obtain an overall minimum in the objective function. Clearly, the model must be interpreted cautiously for sites 10 and 11, but in spite of these difficulties, there are still observations

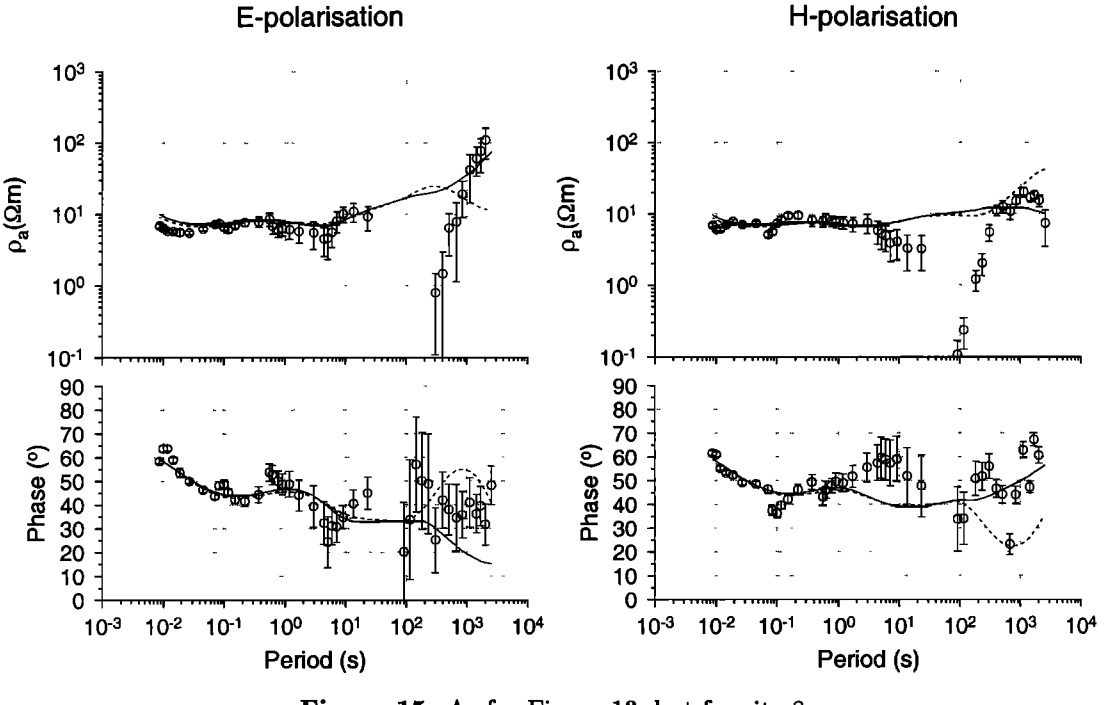

Figure 15. As for Figure 13, but for site 8.

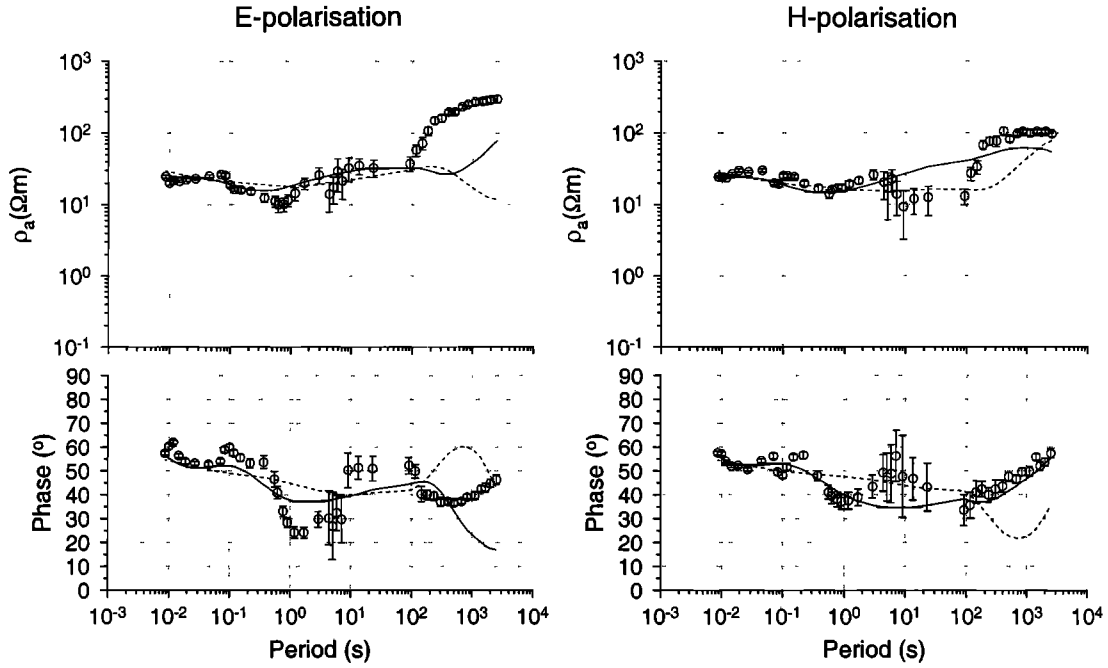

Figure 16. As for Figure 13, but for site 10.

that can be made. The Mana Pools basin deepens from south to north until it encounters the northern escarpment, which has a large resistivity contrast with the basin. The southern escarpment fault seems to represent a smaller resistivity change, and its effect on the data is much less pronounced. It appears to dip steeply to the north, which is in agreement with the interpretation of the seismic data by *Hiller and Buttkus* [1996]. Site 11 on the craton has a high-resistivity near-surface zone but, at depths over 2 km, and the difference in resistivity between the cratonic material and the basement beneath the basin is small. The structure of the geoelectric section is in good agreement with that of the seismic method [*Hiller and Buttkus*, 1996] and also supports the interpretation of the Mana Pools basin by OSNZ as a half graben-like basin with an asymmetric cross section and a depocenter offset to the northwest. A schematic model broadly in agreement with both the MT and seismic data is shown in Figure 18. The main discrepancy between the seismic data and the minimum

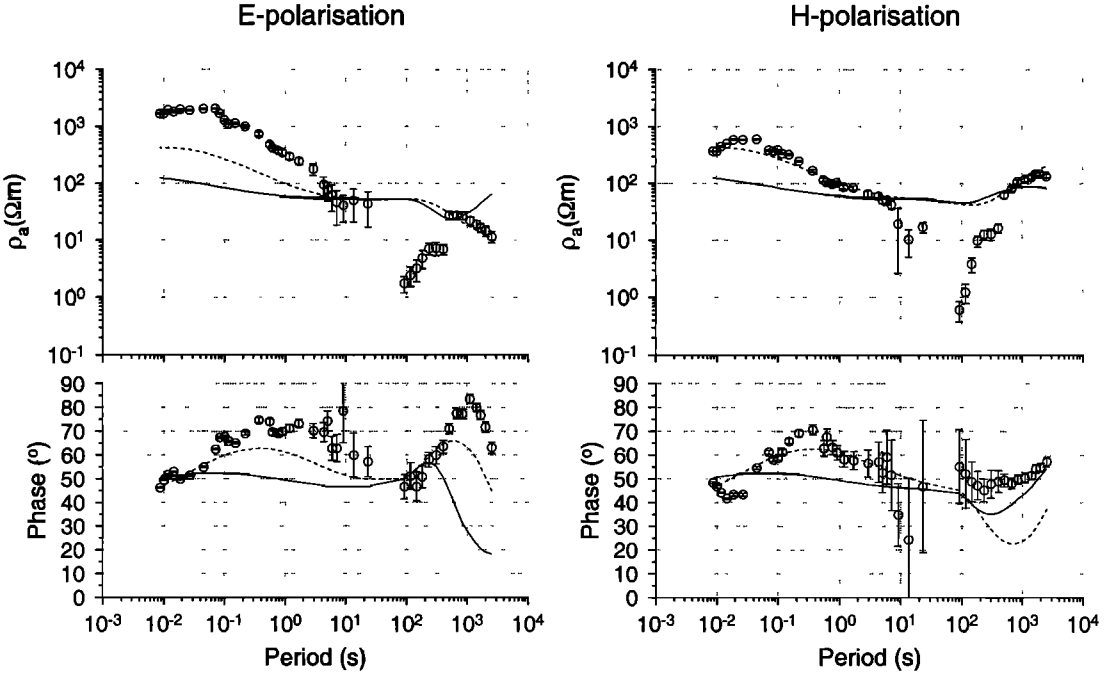

Figure 17. As for Figure 13, but for site 11.

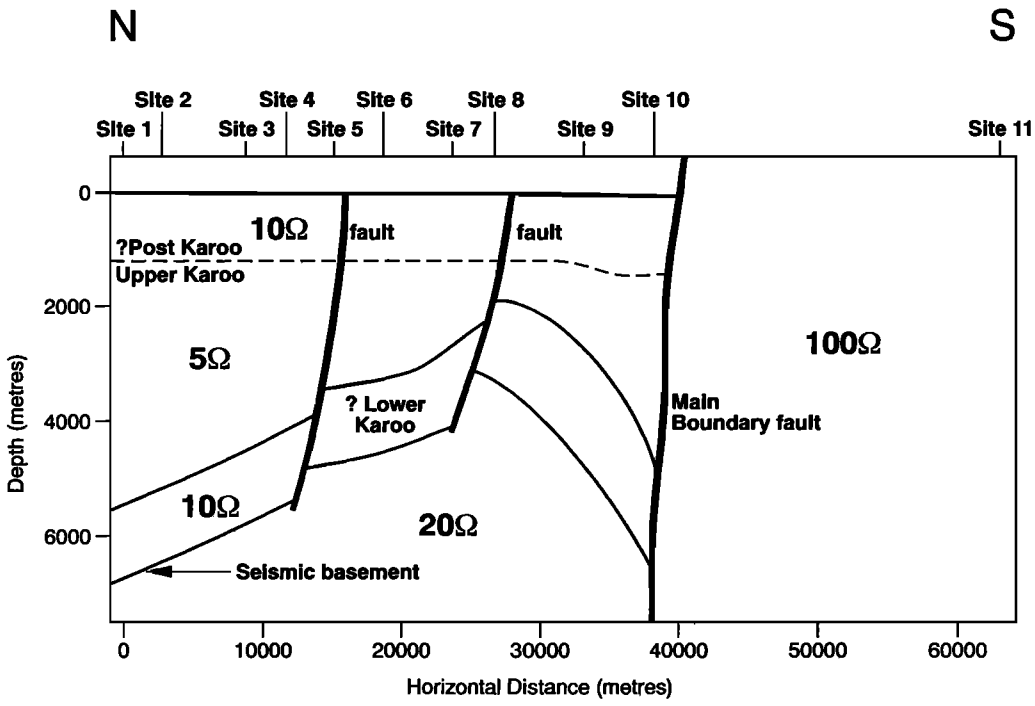

Figure 18. Schematic model for the Mana Pools basin consistent with most features of both the MT and seismic data.

structure resistivity model is in the southern part of the basin. This model and its derivation are further discussed by D. Bailey et al. (Comparison of geoelectric and seismic reflection models of the Zambezi valley basins, submitted to *Geophysical Journal International*, 1999) (hereafter referred to as Bailey et al., submitted manuscript, 1999).

5. Discussion

A two-dimensional resistivity section has been derived for the combined AMT and LMT data sets using the RRI minimum structure routine [*Smith and Booker*, 1991]. Combining the AMT with the recently collected and more sparse LMT data set presents the challenge of finding a modeling approach which ensures a uniform treatment of the entire set, since some sites have data over a considerably larger frequency range than others. This problem has been overcome by the use of different misfit goals at different sites. In all cases, preliminary inversions of both the E and H polarization modes separately are used to determine these goals. The coherency information obtained from the data processing was used to downweight data with values below 80% in the inversion process. This affects a large amount of data, comprising the extreme low-frequency end of the AMT data, data within the dead band, and LMT periods up to 400 s. The appearance of both the apparent resistivity and phase curves within this period range, supported by the ρ^+ work, suggests that they are downward biased to some degree.

The models obtained show three main features. First, there is a well-resolved, low-resistivity body, down to 2 Ωm in approximately the upper 5 km of the valley, terminating at between 5 and 10 km depth. Second, cratonic material is present close to the surface beneath site 11, giving much higher surface resistivities (of ~100 Ωm) in the upper 2 km compared to values in the valley. Third, the resistivity of the model at depths below 10 km is remarkably consistent between the craton and the valley. Although this resistivity is low for basement rocks, at between 20 and 30 Ωm, it is significantly greater than that found at basement depths in other parts of the Damara and Zambezi valley mobile belts (e.g., 1 Ωm in the Lower Zambezi, Figure 5) and probably represents either chemical or tectonic alteration due to metamorphic processes and tectonic disruption during rift formation.

The small resistivity contrast across the escarpment fault separating the Zimbabwe craton in the southern section of the model from the valley means that charge buildup on the fault is small. As a result, its effect on the model response in the valley to the north is also small, and imposing a fault between the craton and the basin barely improves the fit to the LMT data. The degree of separation between the two LMT apparent resistivity curves within the basin increases as the sites are traversed from south to north. This is the reverse of the situation in the Lower Zambezi basin, where the separation in the curves increases from north to south as the resistive southern craton is approached (LKM). The Mana Pools basin is bounded, within Zambia, to the

north by a second escarpment; this feature is required to give an adequate fit to the LMT data.

The conclusions that can be drawn from the resistivity section presented here agree well with the geological evidence and the potential field data presented by OSNZ and also the seismic results of *Hiller and Buttkus* [1996]. The conductor in the upper 7 km of the valley can be identified with the basin using both the seismic data and the depth to basement estimates from potential field data. The resistivity of the basin conductor drops to as low as 2 Ωm, which is unusually small but not unique for a sedimentary succession. An examination of the sensitivity of the data to this conductor shows it to be a robust feature of the model, but we cannot exclude the possibility that it contains thin resistive layers, as has been postulated for the neighboring Lower Zambezi basin due to thin basalt intrusions (LKM).

The basin deepens from south to north, giving an asymmetric profile and implying a depocenter adjacent to the northern margin. This agrees with the interpretations of OSNZ and *Hiller and Buttkus* [1996] (Figure 3); the deepening of the basin adjacent to the Zimbabwe craton in the seismic interpretation is not, however, seen in the MT model. We examine reconciling the seismic and MT models for both the Mana Pools and Lower Zambezi basins in a companion paper (Bailey et al., submitted manuscript, 1999). The large resistivity contrast across the northern escarpment, not sampled seismically and only indirectly by the MT data, suggests that it is likely to represent a faulted contact. The appearance of the resistivity sections is thus consistent with the suggestion of OSNZ that the basin originated as a half graben.

Although the resistivity beneath the Mana Pools basin is extremely low for basement rock, a very conductive body such as that described by *de Beer et al.* [1975, 1976, 1982], *van Zijl and de Beer* [1983] and LKM [see also *Haak and Hutton*, 1986] in the Zambezi and Damara belts is not seen beneath the Mana Pools basin. There is an E polarization phase minimum and an appropriate drop in resistivity across the dead band and at the short-period end of the LMT data which would correspond to the depth of such a feature. However, this section of the data has very low coherency, is believed to be downward biased, and has therefore been severely downweighted. We believe the phase minimum in the dead band is an artifact since the same low values are seen for sites within the valley and site 11 on the escarpment (compare Figures 7 and 8). *Bailey* [1998] performed many sensitivity tests, which unfortunately, do not provide useful constraints on the properties of the possible conductor owing to the poor quality of the data at the relevant periods. However, they do show that an increase in basement resistivity, indicated by the apparent resistivity rise particularly in the E polarization at longer periods, is resolved, so that any conductor here would have significantly lower conductance than that seen elsewhere in southern African mobile belts, where the data are completely opaque to structure beneath the conductor. Elsewhere in the Damara belt, the Kamanjab inlier also has no extremely good conductor beneath [*de Beer et al.*, 1982]; it would be interesting to investigate the geoelectrical structure of the Chewore inliers separating the Mana Pools and Lower Zambezi basins.

Note added in proof. *Ritter et al.* [1999] have recently conducted detailed GDS and MT surveys in the Damara Belt, Namibia, across the conductor. With their tight station spacing, they determined that it comprises two interconnected subvertical features in the midcrust, whose positions correlate with zones of crustal weakness, possibly due to higher fluid content, fault gouge, sulfides, or graphite (which was observed at the surface).

Acknowledgments. We are grateful to NERC, the British Council, and the University of Zimbabwe, who funded this project, and to the many people who helped prepare for and during the field campaign. In particular, we thank Gerhard Schwarz, who provided the electrodes, and the NERC Geophysical Equipment Pool for equipment loans. Thanks also go to Alf Ball and Val Valiant for their technical assistance in the field and Samson Takaedza for his good-natured approach to field assisting. The staff of Mana Pools National Park were extremely helpful, in particular providing storage space for the equipment and access to an electricity generator. Thanks to the Zimbabwean Department of National Parks and Wildlife Management who granted us permits to work in the National Park. The Zimbabwe Geological Survey made the MT data from the Lower Zambezi basin available, and we also thank Keith Fisk at the Ministry of Mines, from whom copies of the seismic sections of the Zambezi valley basins were obtained. Thanks also to two anonymous referees and the Associate Editor, Jeff Love, who made valuable comments on an earlier draft of this paper.

References

Bahr, K., Geological noise in magnetotelluric data: A classification of distortion types, *Phys. Earth Planet. Inter.*, *66*, 24–38, 1991.

Bailey, D. S., Magnetotelluric studies of the Zambezi mobile belt of northern Zimbabwe, Ph.D. thesis, Univ. of Edinburgh, Edinburgh, Scotland, 1998.

Barber, B., The geology and coal potential of the Karoo supergroup and younger rocks in Zimbabwe, Ph.D. thesis, Univ. of Zimbabwe, Harare, 1994.

Booker, J. R., *Documentation for Rapid Relaxation Inversion (RRI 3.1)*, Geophysics, Univ. of Washington, Seattle, 1997.

Bosum, W., and H. Geipel, Reinterpretation of an aeromagnetic profile in the Zambezi valley of Zimbabwe on the basis of magnetotelluric and gravimetric data, *Tech. rep.*, Bundesanstalt für Geowissensch. und Rohstoffe, Hanover, Germany, 1988.

Coward, M. P., and M. C. Daly, Crustal lineaments and shear zones in Africa: Their relationship to plate movements., *Precambrian Res.*, *24*, 27–45, 1984.

Daly, M. C., Crustal shear zones and thrust belts: Their geometry and continuity in central Africa., *Philos. Trans. R. Soc., A317*, 111–128, 1986.

de Beer, J. H., D. I. Gough, and J. S. V. van Zijl, An electrical conductivity anomaly and rifting in southern Africa, *Nature, 255*, 678–680, 1975.

de Beer, J. H., J. S. V. van Zijl, R. M. J. Huyssen, P. L. V. Hugo, S. J. Joubert, and R. Meyer, A magnetometer array study in South - West Africa, Botswana and Rhodesia, *Geophys. J. R. Astron. Soc., 45*, 1–17, 1976.

de Beer, J. H., R. M. J. Huyssen, S. J. Joubert, and J. S. V. van Zijl, Magnetometer array studies and deep Schlumberger soundings in the Damara orogenic belt, South West Africa, *Geophys. J. R. Astron. Soc., 70*, 11–29, 1982.

Egbert, G. D., and J. R. Booker, Robust estimation of geomagnetic transfer functions, *Geophys. J. R. Astron. Soc., 87*, 173–194, 1986.

Groom, R. W., and K. Bahr, Corrections for near surface effects: Decomposition of the magnetotelluric impedance tensor and scaling corrections for regional resistivities: A tutorial, *Surv. Geophys., 13*, 341–379, 1992.

Groom, R. W., and R. C. Bailey, Decomposition of magnetotelluric impedance tensors in the presence of local three-dimensional galvanic distortion, *J. Geophys. Res., 93*, 1913–1925, 1989.

Haak, V., and R. Hutton, Electrical resistivity in continental lower crust, in *The Nature of the Lower Continental Crust*, edited by J. B. Dawson et al., *Spec. Publ. Geol. Soc., 24*, 35–49, 1986.

Hiller, K., and B. Buttkus, Structural style and sedimentary thicknesses in the Zambezi rift valley, Zimbabwe - Investigations of the potential for hydrocarbons, *Z. Angew. Geol., 42*, 132–137, 1996.

Jones, A. G., The problem of current channelling: A critical review, *Geophys. Surveys, 6*, 79–122, 1983.

Livelybrooks, D., R. J. Banks, R. S. Parr, and V. R. S. Hutton, Inversion of electromagnetic induction data for the Iapetus suture zone in the UK, *Phys. Earth Planet. Inter., 81*, 67–84, 1993.

Losecke, W., K. Knödel, and W. Müller, Magnetotelluric survey in the northern Zambezi valley of Zimbabwe, *Tech. Rep. 84.2171.1*, Bundesanstalt für Geowissensch. und Rohstoffe, Hanover, Germany, 1988.

Orpen, J. L., C. J. Swain, C. Nugent, and P. P. Zhou, Wrench-fault and half-graben tectonics in the development of the Palaeozoic Zambezi Karoo basins in Zimbabwe - the Lower Zambezi and Mid-Zambezi basins respectively - and regional implications., *J. Afr. Earth Sci., 8*, 215–229, 1989.

Parker, R. L., The existence of a region inaccessible to magnetotelluric sounding, *Geophys. J. R. atr. Soc., 68*, 165–170, 1982.

Parker, R. L., and J. R. Booker, Optimal one-dimensional inversion and bounding of magnetotelluric apparent resistivity and phase measurements., *Phys. Earth Planet. Inter., 98*, 269–282, 1996.

Ranganai, R. T., Geophysical investigations of the granite-greenstone terrain in the south-central Zimbabwe Archaean Craton, Ph.D. thesis, Univ. of Leeds, Leeds, England, 1995.

Ritter, O., P. Ritter, T. Vietor, and V. Haak, Magnetotelluric investigation of the Damara Belt in Namibia, *EOS Trans. AGU. supp. (December), 80*, 293, 1999.

Smith, J. T., and J. R. Booker, Rapid inversion of two- and three-dimensional magnetotelluric data, *J. Geophys. Res., 96*, 3905–3922, 1991.

Swift, C. M., A magnetotelluric investigation of an electrical conductivity anomaly in the southwestern United States., in *Magnetotelluric Methods, Geophys. Reprints Ser.*, vol. 5, edited by K. Vozoff, pp. 156–166, Soc. of Explor. Geophys., Tulsa, Okla., 1967.

van Zijl, J. S. V., Electrical studies of the deep crust in various tectonic provinces of southern Africa, in *The Earth's Crust, Geophys. Monogr. Ser.*, vol. 20, edited by J. G. Heacock, pp. 470–500, AGU, Washington, D.C., 1977.

van Zijl, J. S. V., and J. H. de Beer, Electrical structure of the Damara orogen and its tectonic significance, *Spec. Publ. Geol. Soc. S. Afr., 11*, 369–379, 1983.

Weidelt, P., and P. Kaikkonen, Local 1-D interpretation of magnetotelluric B-polarization impedances, *Geophys. J. Int., 117*, 733–748, 1994.

Whaler, K. A., and T. G. Zengeni, An audiofrequency magnetotelluric traverse across the Mana Pool Basin, northern Zimbabwe, *Geophys. J. Int., 114*, 673–686, 1993.

D. Bailey and K. A. Whaler, Grant Institute, University of Edinburgh, West Mains Road, Edinburgh EH9 3JW, Scotland. (kathy.whaler@ed.ac.uk)

O. Gwavava and T. Zengeni, Physics Department, University of Zimbabwe, PO Box MP167, Mount Pleasant, Harare, Zimbabwe.

P. C. Jones, British Antarctic Survey, High Cross, Madingley Road, Cambridge CB3 0ET, England.

(Received January 14, 1999; revised November 8, 1999; accepted December 10, 1999.)